Quantitative Structure−Activity Relationships for γδ T Cell Activation by Bisphosphonates

John M. Sanders,[†] Subhash Ghosh,[†] Julian M. W. Chan,[†] Gary Meints,[†] Hong Wang,[‡] Amy M. Raker,[‡] Yongcheng Song,[†] Alison Colantino,[†] Agnieszka Burzynska,[§] Pawel Kafarski,[§] Craig T. Morita,[‡] and Eric Oldfield*,[†]

Department of Chemistry, University of Illinois at Urbana-Champaign, 600 South Mathews Avenue, Urbana, Illinois 61801, Department of Internal Medicine, University of Iowa, EMRB 340F, Iowa City, Iowa 52242, and Institute of Organic Chemistry, Biochemistry and Biotechnology, Wroclaw University of Technology, Wroclaw, Poland

Received August 5, 2003

γδ T cells are the first line of defense against many infectious organisms and are also involved in tumor cell surveillance and killing. They are stimulated by a broad range of small, phosphorus-containing antigens (phosphoantigens) as well as by the bisphosphonates commonly used in bone resorption therapy, such as pamidronate and risedronate. Here, we report the activation of γδ T cells by a broad range of bisphosphonates and develop a pharmacophore model for γδ T cell activation, in addition to using a comparative molecular similarity index analysis (CoMSIA) approach to make quantitative relationships between γδ T cell activation by bisphosphonates and their three-dimensional structures. The CoMSIA analyses yielded R^2 values of ∼0.8−0.9 and q^2 values of ∼0.5−0.6 for a training set of 45 compounds. Using an external test set, the activities (IC_{50} values) of 16 compounds were predicted within a factor of 4.5, on average. The CoMSIA fields consisted of ∼40% hydrophobic, ∼40% electrostatic, and ∼20% steric interactions. Since bisphosphonates are known to be potent, nanomolar inhibitors of the mevalonate/isoprene pathway enzyme farnesyl pyrophosphate synthase (FPPS), we also compared the pharmacophores for γδ T cell activation with those for FPPS inhibition, using the Catalyst program. The pharmacophores for γδ T cell activation and FPPS inhibition both consisted of two negative ionizable groups, a positive charge feature and an endocyclic carbon feature, all having very similar spatial dispositions. In addition, the CoMSIA fields were quite similar to those found for FPPS inhibition by bisphosphonates. The activities of the bisphosphonates in γδ T cell activation were highly correlated with their activities in FPPS inhibition: $R = 0.88$, $p = 0.002$, versus a human recombinant FPPS ($N = 9$ compounds); $R = 0.82$, $p < 0.0001$, for an expressed *Leishmania major* FPPS ($N = 45$ compounds). The bisphosphonate γδ T cell activation pharmacophore differs considerably, however, from that reported previously for γδ T cell activation by phosphoantigens (Gossman, W.; Oldfield, E. *J. Med. Chem.* **2002**, *45*, 4868−4874), suggesting different primary targets for the two classes of compounds. The ability to quite accurately predict the activity of bisphosphonates as γδ T cell activators by using 3D QSAR techniques can be expected to help facilitate the design of additional bisphosphonates for potential use in immunotherapy.

Introduction

γδ T cells expressing the Vγ2Vδ2 (also known as Vγ9Vδ2) T cell receptor (TCR) play an important role in immune system surveillance and defense.[1−4] They recognize, and are activated by, several phosphorus-containing bacterial and protozoan metabolites[5−10] ("phosphoantigens"), such as (*E*)-4-hydroxy-3-methyl-but-2-enyl pyrophosphate (HMBPP, **1**), by synthetic phosphoantigens, such as the bromohydrin of isopentenyl pyrophosphate (Phosphostim, **2**; refs 11 and 12), and by the bisphosphonate drugs commonly used in bone resorption therapy.[13,14] This activation by synthetic drug or drug-like molecules has led to the idea that γδ T cell activation may be used in the immunotherapy of some forms of cancer,[15,16] in the immunotherapy of infectious diseases,[13] and, potentially, in vaccine development.[17] However, the detailed molecular basis for triggering γδ T cell stimulation by phosphoantigens and bisphosphonates is unclear.

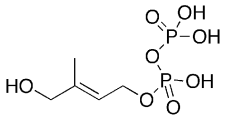

1

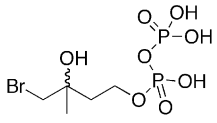

2

There have been a number of theories as to the molecular target(s) of these molecules. For example, Hintz et al.[9] and Allison et al.[18] have proposed that the most potent γδ T cell stimulators, HMBPP and Phosphostim, may bind directly to the γδ T cell receptor, but to date, no such binding has been demonstrated, and indeed, given the likely involvement of presenting molecules in γδ T cell activation, such direct binding may be difficult to observe, since it could be relatively weak. In other work, Thompson et al.[19] have proposed

* To whom correspondence should be addressed. Phone: (217) 333-3374. Fax: (217) 244-0997. E-mail: eo@chad.scs.uiuc.edu.
[†] University of Illinois at Urbana-Champaign.
[‡] University of Iowa.
[§] Wroclaw University of Technology.

10.1021/jm0303709 CCC: $27.50
Published on Web 12/16/2003

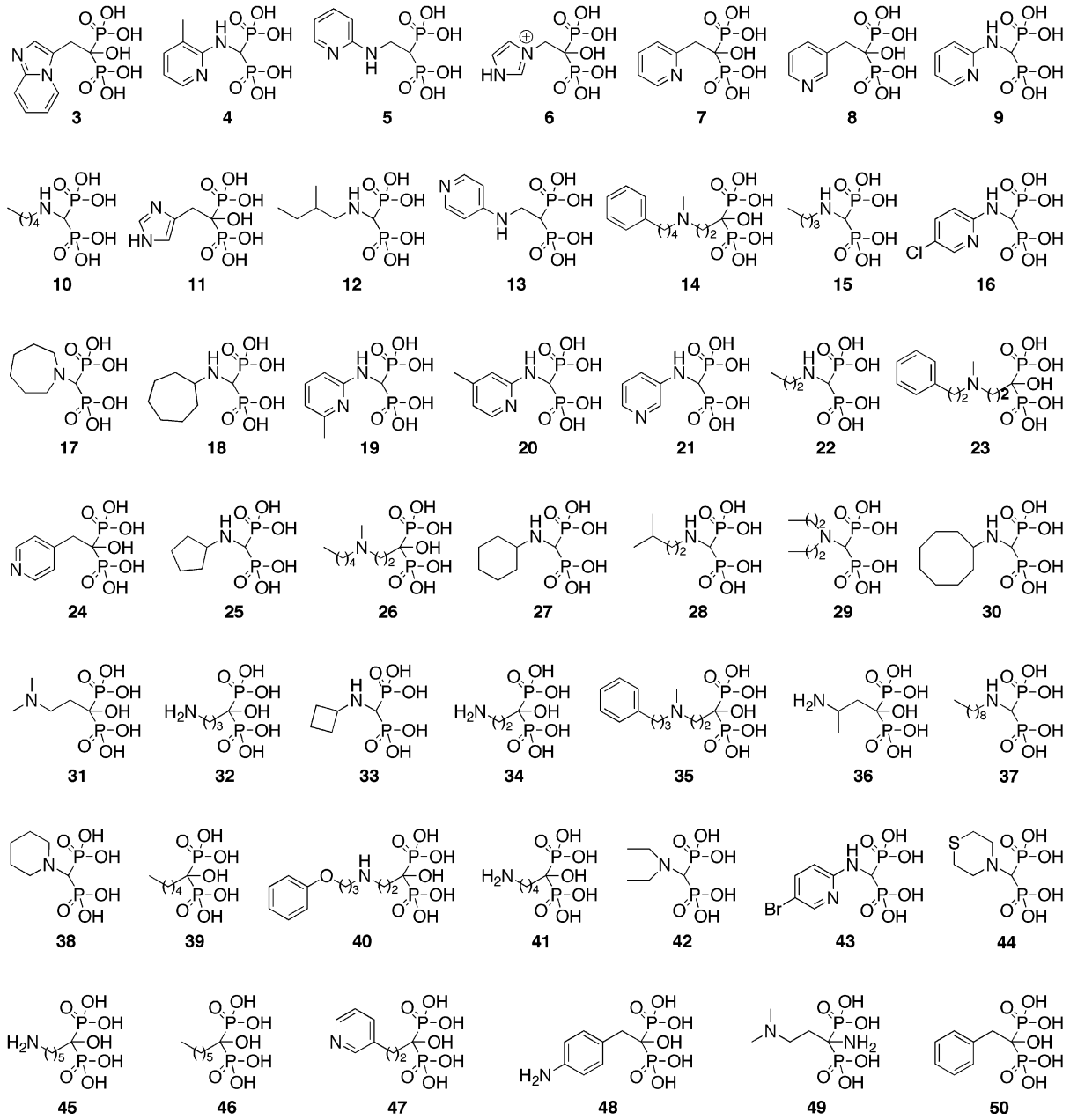

Figure 1. Structures of the training set bisphosphonates investigated as $\gamma\delta$ T cell activators.

that the bisphosphonate zoledronate acts by inhibiting the mevalonate/isoprene biosynthesis pathway enzyme farnesyl pyrophosphate synthase (FPPS), which would lead to elevation of isopentenyl pyrophosphate (IPP) levels, and IPP has also been suggested by Gober et al. to be important in recognition of Daudi tumor cells by $\gamma\delta$ T cells.[20] However, the use of statins in the work of Thompson et al. may complicate the analysis of their results since statins can have multiple targets in immune modulation,[21] and the effects of the lack of β_2-microglobulin in Daudi tumor cells may also be very important in tumor cell recognition.[22] Nevertheless, what is clear is that $\gamma\delta$ T cells are in fact stimulated by bisphosphonates at low micromolar levels. Here, we report the results of our studies of the stimulation of $\gamma\delta$ T cells by a diverse library of bisphosphonates and the use of 3D QSAR (comparative molecular similarity index analysis, CoMSIA, and Catalyst pharmacophore modeling) techniques[23,24] to analyze $\gamma\delta$ T cell stimulation. We make a quantitative comparison between $\gamma\delta$ T cell activation and FPPS inhibition by bisphosphonates, show that 3D QSAR modeling has predictive utility for $\gamma\delta$ T cell activation by bisphosphonates, and, in addition, compare the pharmacophores for $\gamma\delta$ T cell activation by bisphosphonates and phosphoantigens, demonstrating the different chemical natures of the two targets.

Materials and Methods

Computational Aspects. To begin to relate the $\gamma\delta$ T cell stimulation activity of bisphosphonates to their 3D chemical structures, we used two computational chemistry methods commonly used in drug design: comparative molecular similarity index analysis (CoMSIA; ref 23) and Catalyst pharmacophore modeling.[24] The CoMSIA method calculates similarity indices between a molecule and a series of probes (e.g., hydrophobic, electrostatic, and steric) and correlates differences in the indices with activity, while pharmacophore

Table 1. Experimental (IC_{50} and pIC_{50}) and CoMSIA-Predicted (pIC_{50}) Values for Bisphosphonates in Stimulating TNF-α Release in γδ T Cells and Statistical Results for the CoMSIA Models Built Using Individual Observed Maximum TNF-α Release Data

	exptl activity		predicted pIC_{50}	
compd[a]	IC_{50} (μM)	pIC_{50}	GM charges training set	MSK charges training set
3	4.1	5.39	5.34	5.16
4	4.3	5.36	5.11	5.13
5	4.8	5.31	5.38	5.47
6	5.2	5.28	5.02	5.10
7	5.7	5.24	5.14	5.07
8	6.9	5.16	5.18	5.06
9	7.4	5.13	5.02	5.16
10	7.8	5.11	4.85	4.64
11	7.8	5.11	5.05	5.17
12	9.0	5.05	4.97	4.76
13	9.9	5.00	4.70	4.86
14	9.9	5.00	5.02	4.87
15	10	4.99	4.84	4.72
17	11	4.95	4.55	4.51
18	11	4.94	4.61	4.50
19	12	4.92	4.81	5.00
20	13	4.90	5.10	5.08
21	14	4.84	4.93	5.08
22	18	4.74	4.72	4.76
23	19	4.71	4.82	4.69
24	22	4.67	5.05	5.03
25	25	4.60	4.47	4.55
26	31	4.50	4.58	4.49
27	40	4.40	4.58	4.58
28	40	4.40	4.96	4.73
29	41	4.39	4.09	4.28
30	44	4.36	4.66	4.60
31	46	4.33	4.52	4.51
32	53	4.27	4.26	4.40
33	56	4.25	4.35	4.47
34	62	4.21	4.17	4.43
35	63	4.20	4.13	4.10
36	63	4.20	4.05	4.21
37	66	4.18	4.13	4.05
38	66	4.18	4.33	4.38
39	90	4.04	3.87	3.85
40	98	4.01	3.91	3.95
41	102	3.99	4.03	3.86
42	132	3.88	4.08	4.28
44	190	3.72	4.16	4.23
45	196	3.71	3.93	3.71
46	213	3.67	3.86	3.77
47	228	3.64	3.64	3.78
48	251	3.60	3.31	3.33
50	395	3.40	3.66	3.60
	R^2[b]		0.85	0.83
	F-ratio[c]		44.67	48.36
	P value[d]		<0.0001	<0.0001
	q^2[e]		0.49	0.53
	N_{opt}[f]		5	4
	N[g]		45	45
	field contributions			
	hydrophobic		0.405	0.427
	electrostatic		0.380	0.371
	steric		0.215	0.201

[a] Compound structures are shown in Figure 1. The IC_{50} values for **16**, **43,** and **49** (11, 154, and 371 μM) were not included in the CoMSIA analysis, due to the uncertainties in the side chain protonation state described previously (ref 25), but were included in the FPPS inhibition activity correlations (Figure 4). [b] Correlation coefficient. [c] $R^2/(1 - R^2)$, weighted so that the fewer the explanatory properties and the more the values of the target property, the higher the F-ratio (ref 29). [d] P value, from the Prism program (ref 44). [e] Cross-validated correlation coefficient after the leave-one-out procedure. [f] Optimal number of principal components. [g] Number of compounds.

Table 2. Experimental (IC_{50} and pIC_{50}) and CoMSIA-Predicted (pIC_{50}) Values for Bisphosphonates in Stimulating TNF-α Release in γδ T Cells and Statistical Results for the CoMSIA Models Built Using a Constrained Maximum TNF-α Release of 2700 pg/mL

	exptl activity		predicted pIC_{50}	
compd[a]	IC_{50} (μM)	pIC_{50}	GM charges training set	MSK charges training set
4	4.9	5.31	4.98	5.04
7	5.6	5.25	5.11	5.09
8	6.2	5.21	5.11	5.14
6	7.3	5.14	4.72	4.93
3	8.0	5.10	5.37	5.26
11	12	4.92	4.66	5.07
15	13	4.89	4.46	4.41
17	13	4.89	4.32	4.46
5	14	4.84	4.98	5.11
20	14	4.84	4.90	4.86
18	15	4.83	4.54	4.53
9	16	4.81	4.72	4.77
13	16	4.79	4.44	4.75
14	16	4.79	4.90	4.83
12	19	4.71	4.79	4.82
24	21	4.68	4.97	5.08
23	23	4.64	4.75	4.68
21	24	4.62	4.73	4.81
19	28	4.55	4.30	4.18
26	31	4.51	4.49	4.40
22	35	4.46	4.32	4.35
10	41	4.39	4.43	4.25
27	47	4.33	4.46	4.48
28	47	4.33	4.79	4.62
32	52	4.28	4.00	3.98
25	55	4.26	4.20	4.22
29	83	4.08	3.49	3.62
36	110	3.96	3.44	3.32
30	110	3.96	4.61	4.56
31	112	3.95	4.18	4.12
35	121	3.92	3.96	3.79
38	122	3.92	3.90	3.97
33	127	3.90	3.92	3.91
40	143	3.85	3.90	3.81
37	169	3.77	3.75	3.66
41	213	3.67	3.82	3.56
45	503	3.30	3.64	3.53
44	597	3.22	3.63	3.57
47	917	3.04	3.01	3.21
34	941	3.03	3.51	3.44
39	1612	2.79	2.83	2.89
46	2111	2.68	2.79	2.75
50	2818	2.55	2.71	2.62
42	2906	2.54	3.29	3.21
48	19939	1.70	1.40	1.60
	R^2[b]		0.87	0.90
	F-ratio[c]		53.07	67.51
	P value[d]		<0.0001	<0.0001
	q^2[e]		0.57	0.64
	N_{opt}[f]		5	5
	N[g]		45	45
	field contributions			
	hydrophobic		0.357	0.387
	electrostatic		0.429	0.387
	steric		0.214	0.226

[a] Compound structures are shown in Figure 1. The IC_{50} values for **16**, **43**, and **49** (12, 674, and 11210 μM) were not included in the CoMSIA analysis, due to the uncertainties in the side chain protonation state described previously (ref 25). [b] Correlation coefficient. [c] $R^2/(1 - R^2)$, weighted so that the fewer the explanatory properties and the more the values of the target property, the higher the F-ratio (ref 29). [d] P value, from the Prism program (ref 44). [e] Cross-validated correlation coefficient after the leave-one-out procedure. [f] Optimal number of principal components. [g] Number of compounds.

modeling (using the Catalyst program) correlates activity with the presence of chemical features (such as hydrogen bond donors, negative ionizable groups, etc.) and is particularly useful in examining the spatial arrangements of these features. Both approaches have recently been successfully applied by us to analyze the inhibitory activity of bisphosphonates with an FPPS from *Leishmania major*,[25] a geranylgeranyl pyrophosphate synthase,[26] in *Trypanosoma brucei* growth inhibition[27] and in bone resorption.[28]

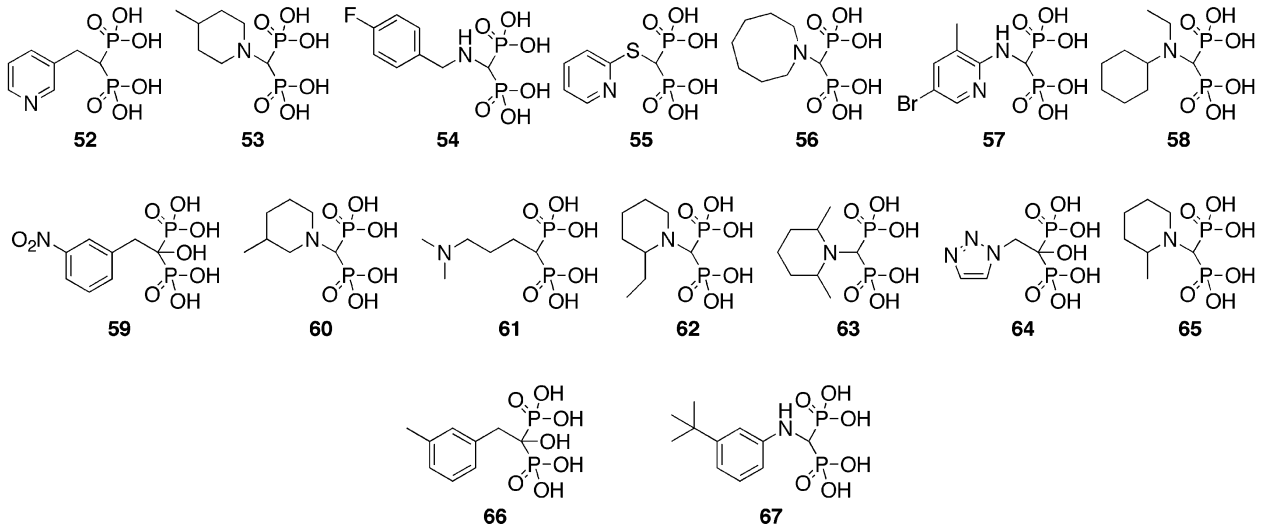

Figure 2. Structures of the external test set bisphosphonates investigated as $\gamma\delta$ T cell activators. In most cases, these test set compounds were synthesized and tested after the training set results had been obtained.

CoMSIA analyses were performed using default settings in the Sybyl 6.9 program.[29] Molecular mechanics minimizations using the Tripos force field were carried out in Sybyl 6.9[29] using a convergence criterion requiring a minimum RMS gradient of 0.01 kcal/(mol·Å) at a steepest descent step and an RMS gradient of 0.001 kcal/(mol·Å) at the following Powell and Broyden, Fletcher, Goldfarb, and Shanno (BFGS) steps. Structures were optimized to convergence at each minimization step. Atomic charges for the CoMSIA analyses were determined for the minimized structures by using the Gasteiger−Marsili (GM) method[30] in Sybyl 6.9.[29] In addition, atomic charges for the minimized structures were also calculated using Hartree−Fock theory (the Merz−Singh−Kollman (MSK) method[31,32] in the Gaussian 98 program[33]), employing a 6-31G* basis set. Compounds were aligned to the (H)O−P−C−P−O(H) atoms of zoledronate (**6**; Figure 1) using the Align Database command in Sybyl 6.9. CoMSIA indices were calculated on a rectangular grid containing the aligned molecules by using hydrophobic, electrostatic and steric probes. Donor and acceptor descriptors were not found to be beneficial in the calculations. The atomic coordinates of the models were then used to compute field values at each point of a 3D grid using a grid spacing of 2.00Å. To obtain a quantitative analysis of the dependence of activity on CoMSIA descriptors, a partial least-squares (PLS) analysis was applied, leading to the results shown in Tables 1 and 2. The optimal number of components for each equation was determined using standard error of prediction values and SAMPLS[34] leave-one-out cross-validation statistics.

Pharmacophore modeling techniques were applied to $\gamma\delta$ T cell activation as well as to human recombinant FPPS inhibition using the HipHop module in Catalyst 4.8.[24] The HipHop algorithm permits a common feature approach to pharmacophore modeling, in which the spatial dispositions of the features common to a group of highly active compounds are related. The TNF-α release and human recombinant FPPS inhibition training sets included up to 256 "best quality" conformations of each of the most active cyclic compounds, built using the Confirm module in Catalyst 4.8.[24] Pharmacophore construction proceeded using a superposition error $S = 0.1$, a spacing value of 220 pm, and default values for the other HipHop variables.[24] Two negative ionizable features, one positive charge feature, and one custom endocyclic carbon feature were used to construct the pharmacophores. The custom-built endocyclic carbon (which identifies any carbon atom that is contained in a ring) was necessary since no default Catalyst feature could account for the variety of ring types present in the training sets.

Synthetic Aspects. The syntheses of the bisphosphonates investigated (**3**−**51**, **53**−**67**; Figures 1 and 2) used methods which are described in more detail elsewhere.[25,26,35−42] **52** was prepared using the following route: **31** and **49** were from Gador

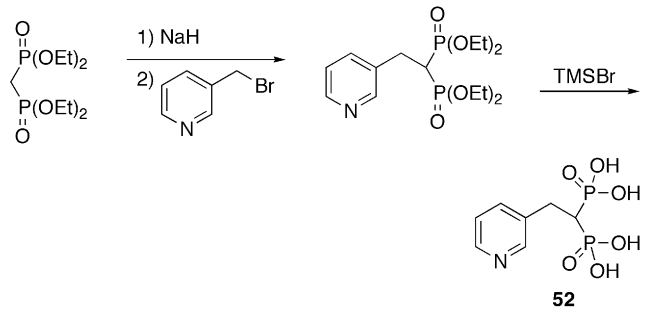

S.A. (Buenos Aires) and were a gift from Teresita Bellido at the University of Arkansas for Medical Sciences. Most compounds investigated were available from previous work.[26,27,37,38] All compounds not previously reported, with the exception of those noted below, had experimental H/C/N analyses that agreed within 0.4% of the calculated values. (**3**) Anal. ($C_9H_{12}N_2P_2O_7 \cdot 0.5H_2O$) C, N, H: calcd, 3.96; found, 3.52. (**6**) Anal. ($C_5H_{10}N_2P_2O_7 \cdot H_2O$) H, C, N: calcd, 9.66; found, 9.25. (**9**) Anal. ($C_6H_{10}N_2P_2O_6 \cdot 0.5H_2O$) C, N, H: calcd, 4.00; found, 3.56. (**13**) Anal. ($C_7H_{11}N_2P_2O_7Na$) C, N, H: calcd, 3.65; found, 4.19. (**22**) Anal. ($C_4H_{13}NP_2O_6 \cdot H_2O$) C, N, H: calcd, 6.02; found, 5.55. (**23**) Anal. ($C_{12}H_{19}NP_2O_7Na_2 \cdot 0.5H_2O$) C, N, H: calcd, 4.96; found, 5.37. (**30**) Anal. ($C_9H_{21}NP_2O_6$) H, N, C: calcd, 35.89; found, 35.44. (**52**) Anal. ($C_7H_{11}NP_2O_6 \cdot 0.5H_2O$) H, N, C: calcd, 30.45; found, 30.88. (**58**) Anal. ($C_9H_{21}NP_2O_6$) H, N, C: calcd, 35.89; found, 35.45. (**64**) Anal. ($C_4H_9N_3P_2O_7 \cdot 1.5H_2O$) C, N, H: calcd, 4.03; found, 3.53. (**66**) Anal. ($C_9H_{13}O_7P_2Na$) H, C: calcd, 33.98; found, 33.42.

***γδ* T Cell Activation and Proliferation.** $\gamma\delta$ T cell activation was assayed by monitoring TNF-α release. For these studies, the Vγ2Vδ2 T cell clone, JN.24,[43] was cultured with glutaraldehyde-fixed CP.EBV B cells. For glutaraldehyde fixation, CP.EBV cells in PBS were reacted with 0.05% glutaraldehyde (EM grade, Sigma, St. Louis, MO) for 15 s at room temperature, followed by exposure to 0.2 M L-lysine (in H_2O at pH 7.4) for 2 min, and then washed three times with PBS. For bisphosphonate stimulation, $(8-10) \times 10^4$ JN.24 T cells were cultured in duplicate in round-bottom 96-well plates with 1×10^5 CP.EBV B cells in the presence of serial half-log dilutions of the various bisphosphonates. Bisphosphonates were added at pH 7.0. Cell supernatants were harvested after 16 h and assayed for TNF-α by sandwich ELISA (R & D Systems, Minneapolis, MN).

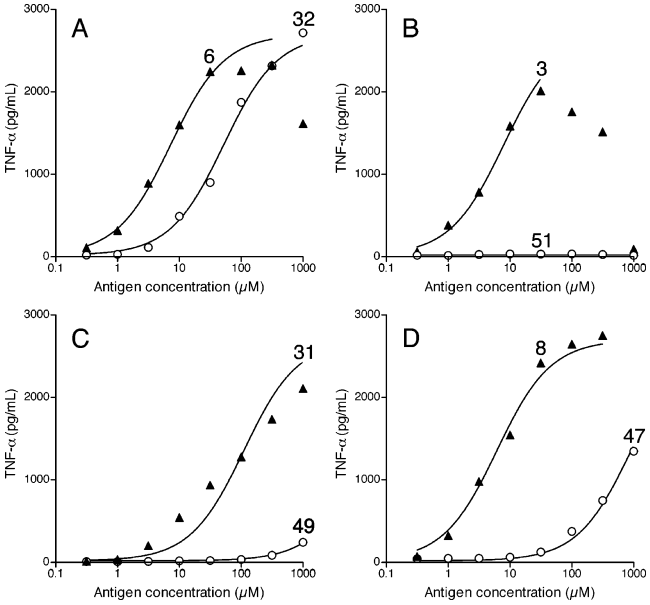

Figure 3. Selected bisphosphonate γδ T cell activation (TNF-α release) results: A, zoledronate (**6**) and alendronate (**32**); B, minodronate (**3**) and isominodronate (**51**); C, olpadronate (**31**) and aminoolpadronate (**49**); D, risedronate (**8**) and homorisedronate (**47**). The data were fitted to a 2700 pg/mL maximal TNF-α release; the 2−3 highest concentration points are omitted from the fitting for **3** and **6,** due to their apparent toxicity.

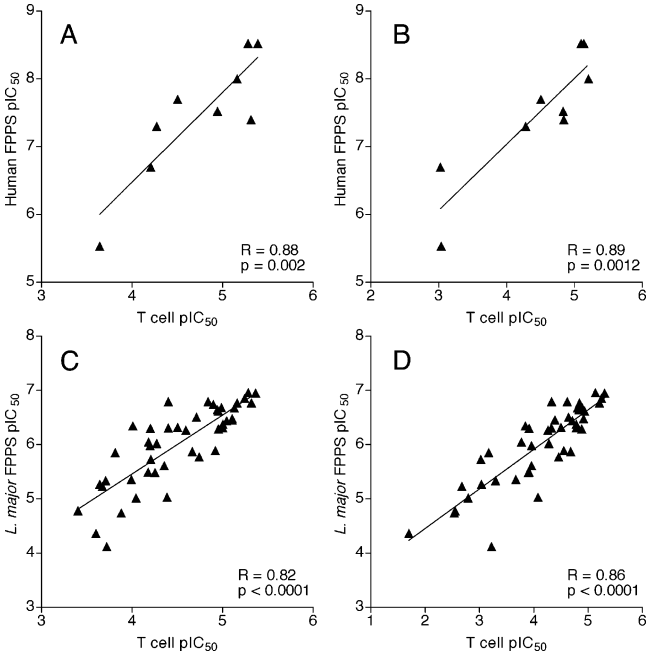

Figure 4. Correlations between γδ T cell activation and FPPS inhibition, by bisphosphonates: A, γδ T cell pIC_{50} (unconstrained fit, Table 1) versus human recombinant FPPS inhibition pIC_{50}, $R = 0.88$, $p = 0.002$; B, as panel A but fitting all experimental data to a maximal TNF-α release value of 2700 pg/mL, $R = 0.89$, $p = 0.0012$; C, as panel A but using *L. major* FPPS inhibition data, $R = 0.82$, $p < 0.0001$; D, as panel C but using a maximal TNF-α release of 2700 pg/mL, $R = 0.86$, $p < 0.0001$.

Results and Discussion

The structures of the bisphosphonates tested in the TNF-α release assay for γδ T cell activation are shown in Figures 1 and 2, and typical experimental dose−response curves for eight compounds (**3**, **6**, **8**, **31**, **32**, **47**, **49**, and **51**) are presented in Figure 3. The Prism 3 program[44] was used to fit the experimental TNF-α release results to a sigmoidal dose−response curve:

$$I = \frac{I_{max} C}{IC_{50} + C} \quad (1)$$

where I is the intensity of the stimulation, I_{max} is the maximum intensity of the stimulation, C is the concentration (μM) of the added bisphosphonate and IC_{50} is the concentration for 50% stimulation (μM). Unlike enzyme inhibition data, a question immediately arises as to how to best define the "maximum" intensity of a stimulation. Two different criteria were tested: using the maximum TNF-α release value observed for each compound as the maximum value (I_{max}), or using the maximum TNF-α value observed for *any* compound (2700 pg/mL) as the maximum (or 100% stimulation) value. As discussed below in more detail, we analyzed the results obtained using both methods but found that there were no differences in the conclusions obtained. In Figure 3, the fits are to eq 1, constrained to a maximum TNF-α release level of 2700 pg/mL, with "toxic" high concentration (>50 μM) points for **3** (minodronate) and **6** (zoledronate) omitted from the fitting.

In Figure 3A, we show stimulation results for two commonly used bone resorption drugs: alendronate (Fosamax, **32**) and zoledronate (Zometa, **6**). The more potent bone resorption drug (and FPPS inhibitor), zoledronate, has about an order of magnitude more activity in γδ T cell stimulation than does alendronate. In Figure 3B−D, we present results for three more pairs of bisphosphonates in which the effects of minor chemical changes are known to abrogate bisphosphonate effects on bone resorption and/or FPPS inhibition. Their structures are shown below: For example, the drugs

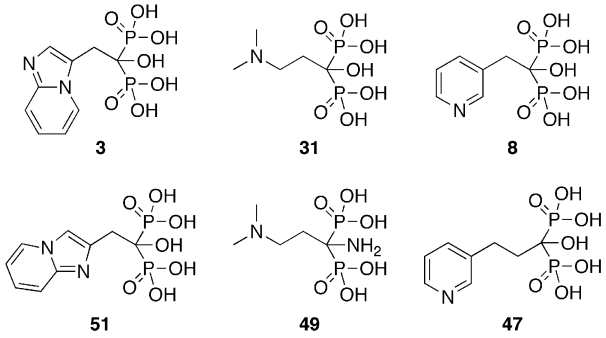

minodronate (**3**), olpadronate (**31**), and risedronate (**8**) (top row) are all potent γδ T cell activators (Figure 3B−D), bone resorption drugs,[35,39,45,46] and FPPS inhibitors.[25,45] However, moving the position of ring alkylation in **3** (to **51**), replacing the OH group by an NH_2 in **31** (to **49**), or adding a CH_2 group to **8** (to **47**) (bottom row) results in the loss of essentially all activity in γδ T cell activation (Figure 3B−D), bone resorption,[39,45,46] or FPPS inhibition.[25,45] While these observations do not, in and of themselves, prove a causal link between FPPS inhibition and γδ T cell activation (as suggested by Thompson et al.[19]), the effects of minor structural changes are very pronounced and do suggest the possibility of such a relationship. To test this possibility

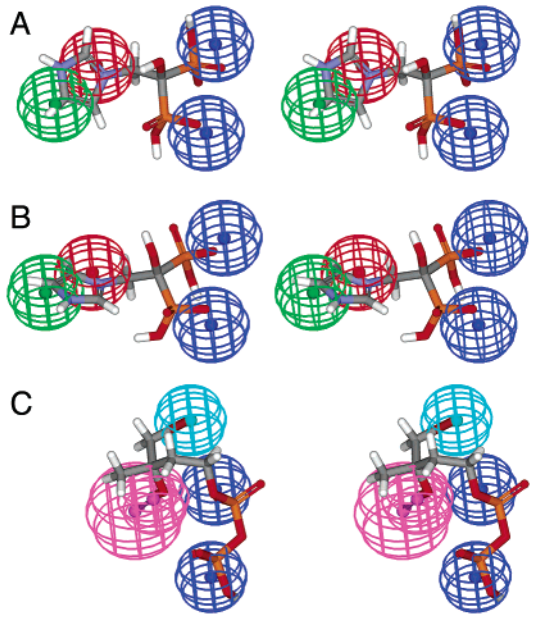

Figure 5. Stereoviews of pharmacophores for $\gamma\delta$ T cell activation and FPPS inhibition obtained using the Viewer Lite program (ref 47): A, model for TNF-α release by bisphosphonates superimposed on zoledronate (**6**), training set composed of the 11 most active, cyclic compounds (constrained fit, Table 2); B, model for human recombinant FPPS inhibition by bisphosphonates superimposed on **6**. Training set composed of the 5 most active, cyclic compounds (from ref 45); C, phosphoantigen pharmacophore (from ref 48) superimposed on Phosphostim (**2**). Key: blue spheres, negative ionizable features; red spheres, positive charge features; green spheres, endocyclic carbon features; cyan sphere, hydrophobic feature; pink spheres, hydrogen bond donor feature.

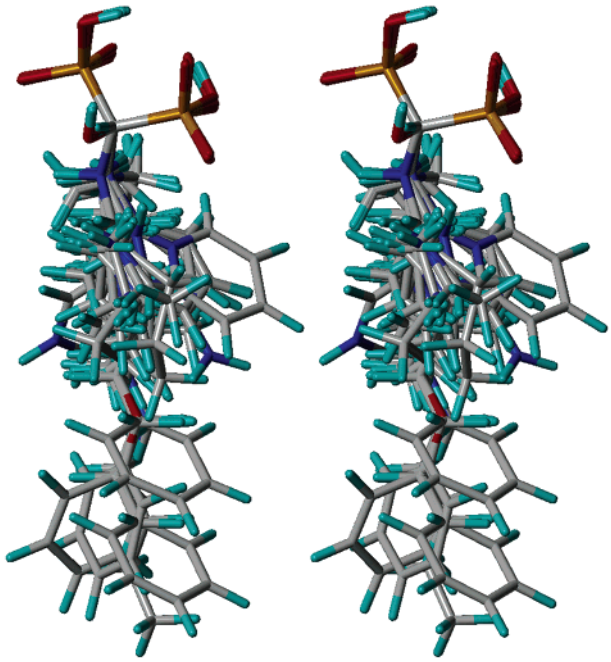

Figure 6. Stereoview of bisphosphonate alignment ($N = 45$ compounds) used in the CoMSIA analyses.

further, we next compared the activities of the bisphosphonates shown in Figure 1 in $\gamma\delta$ T cell activation (using $pIC_{50} = -[\log IC_{50}\ (M)]$ values) with their activities in inhibiting FPPS synthase (again using $pIC_{50} = -[\log IC_{50}\ (M)]$ values) using the Prism 3 program.[44] At present, there are published IC_{50} values for human, recombinant FPPS inhibition[45] for nine of the compounds we have investigated (**3**, **5**, **6**, **8**, **18**, **26**, **32**, **34**,and **47**). These published results are compared in Figure 4A with the TNF-α release results obtained here using data fit to the maximum observed TNF-α release for a given compound. There is a high correlation between the two data sets ($R = 0.88$, $p = 0.002$), and similar results were obtained by using TNF-α release results constrained to the maximum value seen for any compound ($I_{max} = 2700$ pg/mL), Figure 4B ($R = 0.89$ and $p = 0.0012$). A second set of correlations are shown in Figure 4C,D, in which we compare the pIC_{50} values for $\gamma\delta$ T cell activation (TNF-α release) with inhibition results obtained on an expressed *L. major* FPP synthase enzyme.[25] Use of the *L. major* enzyme is expected to introduce some scatter into the correlation since the *L. major* and human enzymes have only 31.7% identity, but since the two FPPS inhibition data sets are highly correlated for the nine bisphosphonates where enzyme inhibition data are available in both systems ($R = 0.92$, $p = 0.0013$, data not shown), this approach seems a reasonable one and does allow us to investigate a more structurally diverse range of bisphosphonates. For the pIC_{50} ($\gamma\delta$ T cell TNF-α release)/pIC_{50} (*L. major* FPPS inhibition) correlations we find $R = 0.82$ and $R = 0.86$ with $p < 0.0001$, for the unconstrained and constrained (2700 pg/mL) data sets, respectively. These results demonstrate that $\gamma\delta$ T cell activation by bisphosphonates is highly correlated with their activity as FPPS inhibitors.

To further investigate the chemical features responsible for $\gamma\delta$ T cell activation, we next used pharmacophore modeling using the Catalyst program.[24] The pharmacophores for $\gamma\delta$ T cell activation and human recombinant FPPS inhibition are shown in Figure 5A,B, respectively. Each pharmacophore hypothesis contained two negative ionizable groups (the bisphosphonate OH groups, shown as blue spheres), an endocyclic carbon feature (green sphere), and a cationic feature (red sphere). The two pharmacophores are very similar, consistent with the observation that the $\gamma\delta$ T cell activation and FPPS enzyme inhibition activity profiles are highly correlated (Figure 4). The pharmacophores shown in Figure 5A,B are, however, very different from the one previously reported for $\gamma\delta$ T cell activation by more classical phosphoantigens, such as **1** and **2**.[48] In that work, $\gamma\delta$ T cell activation by 39 phosphoantigens was investigated, and it was found that the top-scoring pharmacophore hypothesis (Figure 5C), although containing two negative ionizable groups and a hydrophobic feature, lacked the positive charge feature found in all of the highly active, nitrogen-containing bisphosphonates. Instead, a hydrogen bond donor feature was present. Although in this earlier work there were in fact three nitrogen-containing bisphosphonates included in the training set, these compounds were >1000× less active than the most active phosphoantigens, and consequently, they contributed little to the overall pharmacophore hypothesis. Moreover, the Catalyst and molecular field analysis (MFA) hypotheses generated in the previous work, while giving good overall predictions of phosphoantigen activity,[48] were found to be incapable of predicting the current bisphosphonate $\gamma\delta$ T cell activation results. It therefore appears that the primary

targets for bisphosphonates and phosphoantigens acting as γδ T cell activators are different.

To investigate in more detail the structure−activity relationships for bisphosphonates in γδ T cell activation, we next used the CoMSIA method to analyze the γδ T cell (TNF-α release) activation results. The alignment strategy we adopted was basically that which we used in the past to investigate bisphosphonates as inhibitors of a vacuolar pyrophosphatase[49] and *L. major* FPPS,[25] as *T. brucei* growth inhibitors[27] and as bone resorption inhibitors.[28] In brief, zoledronate was used as a shape reference compound, the phosphonate groups were each assigned a single negative charge, and side chain nitrogen atoms were protonated. The overall alignment obtained is shown in Figure 6. In our previous studies, several different bisphosphonate alignments were studied.[27,28] For bisphosphonates containing long side chains, it was found to be desirable to incorporate protein structural information to guide the side chain alignments,[28] but in the present work, since the target is not proven and since there are no extended side chain species, we simply chose to use extended side chains. To begin, we used pIC_{50} values obtained by fitting the experimental TNF-α release results for each compound, unconstrained to any maximal release value, as shown in Table 1 and Figure 3. Two groups of training set calculations were carried out. The first used GM charges,[30] while the second used MSK charges,[31,32] computed by using Hartree−Fock theory (6-31G* basis set) in Gaussian 98.[33] Both methods yielded good R^2 (0.83, 0.85), *F*-ratio (45, 48), and q^2 (0.49, 0.53) results on the $N = 45$ compound training set, Table 1. These results were then further validated by using a data randomization method in which SAMPLS cross-validation[34] was carried out using randomly generated pIC_{50} values in place of the experimentally determined values, as reported previously.[25] For all training sets, this approach gave average q^2_{random} values <0 for 100 randomization runs. The maximum q^2_{random} values obtained using this procedure were all statistically insignificant and substantially lower than the q^2 values obtained with the experimental training sets. These results give confidence that the good training set results, shown graphically in Figure 7A,B, do not occur by chance.

As discussed above, a question arises with the TNF-α release bioassay as to the most appropriate definition of the "IC_{50}" (or equivalently the EC_{50}) for T cell stimulation. That is, should the IC_{50} correspond to 50% of the observed maximum release for a given compound, or should it be 50% of a maximum value—one which might not actually be reached experimentally for a given compound (due, e.g., to toxicity)? To assess whether this question might influence any conclusions of this study, we therefore repeated the calculations shown in Table 1 using pIC_{50} data obtained by fitting the experimental results to a maximum TNF-α release of 2700 pg/mL—a value which is in fact attained by most of the active compounds studied. The IC_{50} and pIC_{50} values so obtained are shown in Table 2. Although there is some scatter evident when these pIC_{50} results are compared with those shown in Table 1, the pIC_{50} values are still highly correlated with the results shown in Table 1, with an $R^2 = 0.84$ and $p < 0.0001$.

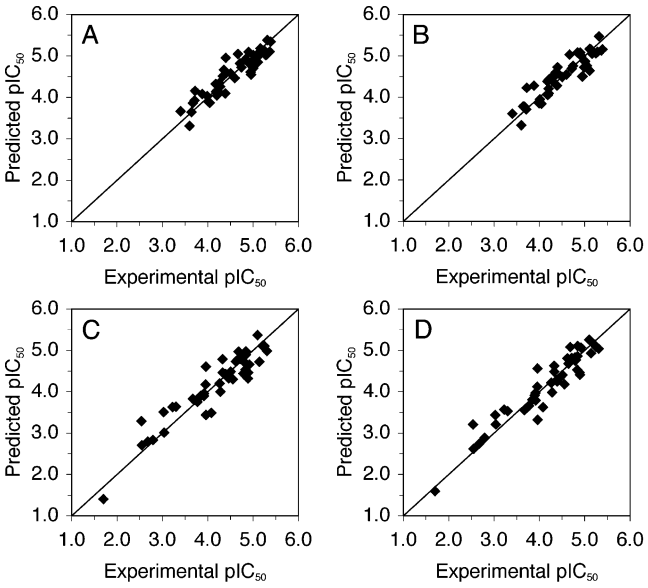

Figure 7. Experimental versus CoMSIA computed pIC_{50} results for γδ T cell activation (TNF-α release) by bisphosphonates: A, training set (Table 1), GM charges, $R^2 = 0.85$, $p < 0.0001$; B, training set (Table 1), MSK charges, $R^2 = 0.83$, $p < 0.0001$; C, training set (Table 2), GM charges, $R^2 = 0.87$, $p < 0.0001$; D, training set (Table 2), MSK charges, $R^2 = 0.90$, $p < 0.0001$.

Using this set of pIC_{50} values, we repeated the training set CoMSIA calculations, again using both GM and MSK charge sets. The computed results are shown in Table 2 and are presented graphically in Figure 7C,D. The R^2, *F*-ratio, and q^2 values were generally slightly better than those shown in Table 1, suggesting most likely that there is a common "maximal" bisphosphonate stimulation which can be obtained with γδ T cells. The CoMSIA fields derived by using either GM or MSK charges were found to be very similar and consist of hydrophobic (∼39%), electrostatic (∼39%), and steric (∼21%) interactions. These values are each within ∼5% of those obtained using a similar set of compounds acting as inhibitors of the *L. major* FPPS enzyme.[25] The hydrophobic field, Figure 8A (MSK charges), is generally unremarkable, with a favorable hydrophobic feature located on the aromatic ring. Also, as expected, the electrostatic field (Figure 8B) places a positive charge region over the distal ring N atom. The favored steric field feature (Figure 8C, green) closely maps the favored hydrophobic field feature (Figure 8A, yellow), while the disfavored steric field feature (Figure 8C, yellow) maps to a long-chain compound having low activity, due most likely to steric repulsion with the putative protein target. The locations of these CoMSIA field features are also quite similar to those found for FPPS inhibition by bisphosphonates[25] and in bone resorption inhibition by bisphosphonates.[28]

We then tested the predictive ability of the CoMSIA approach using an external test set in which the activities of 16 compounds that were not included in any training set calculations were computed from the training set equation (using MSK charges and experimental data fit to the theoretical maximum TNF-α release of 2700 pg/mL, the combination which gave the best training set statistics, Figure 7D). The experimental and predicted test set results are given in Table 3 and shown graphically in Figure 9 and are quite predictive (a factor

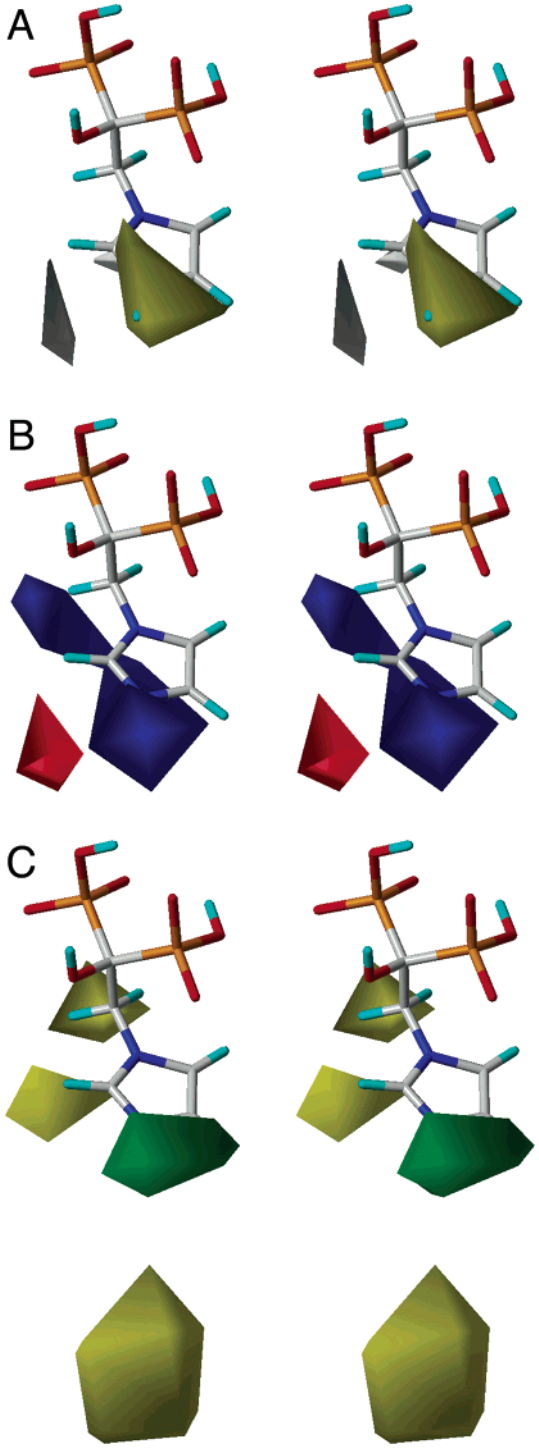

Figure 8. Stereoviews of CoMSIA field contours for $\gamma\delta$ T cell stimulation by bisphosphonates shown superimposed on zoledronate (**6**). A, hydrophobic field (yellow, hydrophobic interaction favored; white, hydrophobic interaction disfavored); B, electrostatic field (blue, positive charge favored; red, negative charge favored); C, steric field (green, bulky group favored; yellow, bulky group disfavored).

of 4.5 error over ~4 orders of magnitude in experimental activity, $R^2 = 0.65$, $p = 0.0002$).

Conclusions. The results we have described above are of interest for a number of reasons. First, we have obtained the most comprehensive data so far on $\gamma\delta$ T cell activation by bisphosphonates. Second, we find that the overall pattern of activity of bisphosphonates in $\gamma\delta$ T cell activation generally mirrors their activity as

Table 3. Experimental (IC_{50} and pIC_{50}) and CoMSIA-Predicted (pIC_{50}) Values for Bisphosphonates in Stimulating TNF-α Release in $\gamma\delta$ T Cells Using a Constrained Maximum TNF-α Release of 2700 pg/mL

	exptl activity		predicted pIC_{50}
compd[a]	IC_{50} (μM)	pIC_{50}	MSK charges test set
52	10	4.98	5.61
53	24	4.63	4.08
54	63	4.20	3.84
55	67	4.17	5.57
56	68	4.17	4.40
57	72	4.14	4.54
58	103	3.99	3.60
59	110	3.96	5.00
60	348	3.46	3.98
61	400	3.40	4.21
62	1203	2.92	3.71
63	1648	2.78	3.37
64	2070	2.68	2.47
65	2741	2.56	3.59
66	9015	2.05	2.55
67	25184	1.60	2.84

[a] Compound structures are shown in Figure 2.

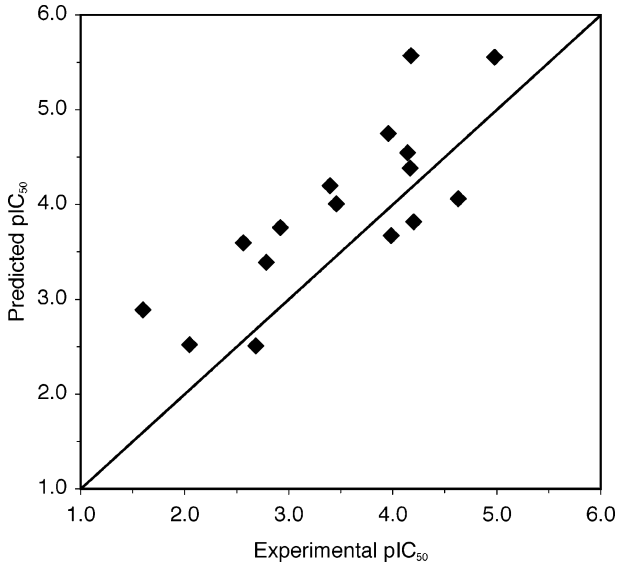

Figure 9. Experimental versus CoMSIA computed pIC_{50} results for $\gamma\delta$ T cell activation (TNF-α release) by test set bisphosphonates. Activity values (Table 3) were computed using MSK charges and the training set equation obtained with MSK charges (Table 2), $R^2 = 0.65$, $p = 0.0002$.

inhibitors of the mevalonate/isoprene pathway enzyme farnesyl pyrophosphate synthase. In particular, the pIC_{50} results for $\gamma\delta$ T cell activation and FPPS inhibition are highly correlated ($R \approx 0.8-0.9$, $p \leq 0.002$). Third, we have used computer modeling (the Catalyst program) to compare the pharmacophores for these bisphosphonates in $\gamma\delta$ T cell activation and FPPS inhibition. The pharmacophores are very similar, but differ from those for $\gamma\delta$ T cell activation by phosphoantigens. The pharmacophores for $\gamma\delta$ T cell activation by bisphosphonates and for FPPS inhibition both contain a positive charge feature which is absent in the phosphoantigen $\gamma\delta$ T cell activation pharmacophore, which, instead, contains a hydrogen bond donor feature (the OH group in **1** or **2**), implying different targets for phosphoantigens and bisphosphonates. Fourth, we have used the CoMSIA approach to make quantitative structure−activity relationship correlations for bisphosphonates acting as $\gamma\delta$

T cell activators. Hydrophobic and electrostatic contributions dominate the CoMSIA fields, and using a training/test set approach, the method was found to have predictive utility (about a factor of 4.5 error in IC_{50} prediction). These results and approaches may be of use in the development of novel bisphosphonates for use in immunotherapy, where very recently it has been shown that pamidronate/IL-2 therapy has potential in treating some hematological malignancies,[16] in addition to providing an intriguing set of correlations among γδ T cell activation, FPPS inhibition and chemical structure.

Acknowledgment. We thank Teresita Bellido at the University of Arkansas for Medical Sciences for providing compounds **31** and **49**. This work was supported in part by the United States Public Health Service (National Institutes of Health Grants GM-50694 and AR-45504). This work was supported by an award from the American Heart Association. J.M.S. is an American Heart Association, Midwest Affiliate Predoctoral Fellow. G.M. is a USPHS NRSA Postdoctoral Fellow (NIH Grant GM-65782).

References

(1) Hayday, A. C. γ,δ Cells: A right time and a right place for a conserved third way of protection. *Annu. Rev. Immunol.* **2000**, *18*, 975−1026.
(2) Bendelac, A.; Bonneville, M. Autoreactivity by design: Innate B and T lymphocytes. *Nat. Rev. Immunol.* **2001**, *1*, 177−185.
(3) Girardi, M.; Oppenheim, D. E.; Steele, C. R.; Lewis, J. M.; Glusac, E.; Filler, R.; Hobby, P.; Sutton, B.; Tigelaar, R. E.; Hayday, A. C. Regulation of cutaneous malignancy by γδ T cells. *Science* **2001**, *294*, 605−609.
(4) Morita, C. T.; Mariuzza, R. A.; Brenner, M. B. Antigen recognition by human γδ T cells: Pattern recognition by the adaptive immune system. *Springer Semin. Immunopathol.* **2000**, *22*, 191−217.
(5) Tanaka, Y.; Sano, S.; Nieves, E.; De Libero, G.; Rosa, D.; Modlin, R. L.; Brenner, M. B.; Bloom, B. R.; Morita, C. T. Nonpeptide ligands for human γδ T cells. *Proc. Natl. Acad. Sci. U.S.A.* **1994**, *91*, 8175−8179.
(6) Tanaka, Y.; Morita, C. T.; Tanaka, Y.; Nieves, E.; Brenner, M. B.; Bloom, B. R. Natural and synthetic non-peptide antigens recognized by human γδ T cells. *Nature* **1995**, *375*, 155−158.
(7) Behr, C.; Poupot, R.; Peyrat, M. A.; Poquet, Y.; Constant, P.; Dubois, P.; Bonneville, M.; Fournié, J. J. *Plasmodium falciparum* stimuli for human γδ T cells are related to phosphorylated antigens of mycobacteria. *Infect. Immun.* **1996**, *64*, 2892−2896.
(8) Morita, C. T.; Lee, H. K.; Leslie, D. S.; Tanaka, Y.; Bukowski, J. F.; Marker-Hermann, E. Recognition of nonpeptide prenyl pyrophosphate antigens by human γδ T cells. *Microbes Infect.* **1999**, *1*, 175−186.
(9) Hintz, M.; Reichenberg, A.; Altincicek, B.; Bahr, U.; Gschwind, R. M.; Kollas, A. K.; Beck, E.; Wiesner, J.; Eberl, M.; Jomaa, H. Identification of (*E*)-4-hydroxy-3-methyl-but-2-enyl pyrophosphate as a major activator for human γδ T cells in *Escherichia coli*. *FEBS Lett.* **2001**, *509*, 317−322.
(10) Feurle, J.; Espinosa, E.; Eckstein, S.; Pont, F.; Kunzmann, V.; Fournié, J. J.; Herderich, M.; Wilhelm, M. *Escherichia coli* produces phosphoantigens activating human γδ T cells. *J. Biol. Chem.* **2002**, *277*, 148−154.
(11) Belmant, C.; Espinosa, E.; Halary, F.; Tang, Y.; Peyrat, M. A.; Sicard, H.; Kozikowski, A.; Buelow, R.; Poupot, R.; Bonneville, M.; Fournié, J. J. A chemical basis for selective recognition of nonpeptide antigens by human γδ T cells. *FASEB J.* **2000**, *14*, 1669−1670.
(12) Espinosa, E.; Belmant, C.; Pont, F.; Luciani, B.; Poupot, R.; Romagne, F.; Brailly, H.; Bonneville, M.; Fournié, J. J. Chemical synthesis and biological activity of bromohydrin pyrophosphate, a potent stimulator of human γδ T cells. *J. Biol. Chem.* **2001**, *276*, 18337−18344.
(13) Wang, L.; Kamath, A.; Das, H.; Li, L.; Bukowski, J. F. Antibacterial effect of human Vγ2Vδ2 T cells *in vivo*. *J. Clin. Invest.* **2001**, *108*, 1349−1357.
(14) Das, H.; Wang, L.; Kamath, A.; Bukowski, J. F. Vγ2Vδ2 T-cell receptor-mediated recognition of aminobisphosphonates. *Blood* **2001**, *98*, 1616−1618.
(15) Sicard, H.; Al Saati, T.; Delsol, G.; Fournié, J. J. Synthetic phosphoantigens enhance human Vγ9Vδ2 T lymphocytes killing of non-Hodgkin's B lymphoma. *Mol. Med.* **2001**, *7*, 711−722.
(16) Wilhelm, M.; Kunzmann, V.; Eckstein, S.; Reimer, P.; Weissinger, F.; Ruediger, T.; Tony, H. P. γδ T cells for immune therapy of patients with lymphoid malignancies. *Blood* **2003**, *102*, 200−206.
(17) Belmant, C.; Fournié, J. J.; Bonneville, M.; Peyrat, M. A. Nouveaux composés phosphohalohydrines, procédé de fabrication et applications. French Patent FR2782721, March 3, 2000.
(18) Allison, T. J.; Winter, C. C.; Fournié, J. J.; Bonneville, M.; Garboczi, D. N. Structure of a human γδ T-cell antigen receptor. *Nature* **2001**, *411*, 820−824.
(19) Thompson, K.; Gordon, S. A.; Rogers, M. J. N-bisphosphonates stimulate proliferation of γδ-T cells in human PBMC cultures by inhibiting the mevalonate pathway: Clarification of the acute phase response. *J. Bone Miner. Res.* **2002**, *17*, F249.
(20) Gober, H. J.; Kistowska, M.; Angman, L.; Jeno, P.; Mori, L.; De Libero, G. Human T cell receptor γδ cells recognize endogenous mevalonate metabolites in tumor cells. *J. Exp. Med.* **2003**, *197*, 163−168.
(21) Weitz-Schmidt, G.; Welzenbach, K.; Brinkmann, V.; Kamata, T.; Kallen, J.; Bruns, C.; Cottens, S.; Takada, Y.; Hommel, U. Statins selectively inhibit leukocyte function antigen-1 by binding to a novel regulatory integrin site. *Nat. Med.* **2001**, *7*, 687−692.
(22) Rothenfusser, S.; Buchwald, A.; Kock, S.; Ferrone, S.; Fisch, P. Missing HLA class I expression on Daudi cells unveils cytotoxic and proliferative responses of human γδ T lymphocytes. *Cell Immunol.* **2002**, *215*, 32−44.
(23) Klebe, G.; Abraham, U.; Mietzner, T. Molecular similarity indices in a comparative analysis (CoMSIA) of drug molecules to correlate and predict their biological activity. *J. Med. Chem.* **1994**, *37*, 4130−4146.
(24) *Catalyst*, version 4.8; Accelrys Inc., 9685 Scranton Rd., San Diego, CA 92121.
(25) Sanders, J. M.; Gómez, A. O.; Mao, J.; Meints, G. A.; Van Brussel, E. M.; Burzynska, A.; Kafarski, P.; González-Pacanowska, D.; Oldfield, E. 3-D QSAR investigations of the inhibition of *Leishmania major* farnesyl pyrophosphate synthase by bisphosphonates. *J. Med. Chem.* **2003**, *46*, 5171−5183.
(26) Szabo, C. M.; Matsumura, Y.; Fukura, S.; Martin, M. B.; Sanders, J. M.; Sengupta, S.; Cieslak, J. A.; Loftus, T. C.; Lea, C. R.; Lee, H. J.; Koohang, A.; Coates, R. M.; Sagami, H.; Oldfield, E. Inhibition of geranylgeranyl diphosphate synthase by bisphosphonates and diphosphates: a potential route to new bone antiresorption and antiparasitic agents. *J. Med. Chem.* **2002**, *45*, 2185−2196.
(27) Martin, M. B.; Sanders, J. M.; Kendrick, H.; de Luca-Fradley, K.; Lewis, J. C.; Grimley, J. S.; Van Brussel, E. M.; Olsen, J. R.; Meints, G. A.; Burzynska, A.; Kafarski, P.; Croft, S. L.; Oldfield, E. Activity of bisphosphonates against *Trypanosoma brucei rhodesiense*. *J. Med. Chem.* **2002**, *45*, 2904−2914.
(28) Kotsikorou, E.; Oldfield, E. A quantitative structure activity relationship and pharmacophore modeling investigation of aryl-X and heterocyclic bisphosphonates as bone resorption agents. *J. Med. Chem.* **2003**, *46*, 2932−2944.
(29) *SYBYL*, version 6.9; Tripos Inc., 1699 South Hanley Rd., St. Louis, MO 63144.
(30) Gasteiger, J.; Marsili, M. Iterative partial equalization of orbital electronegativity − a rapid access to atomic charges. *Tetrahedron* **1980**, *36*, 3219−3228.
(31) Besler, B. H.; Merz, K. M., Jr.; Kollman, P. A. Atomic charges derived from semiempirical methods. *J. Comput. Chem.* **1990**, *11*, 431−439.
(32) Singh, U. C.; Kollman, P. A. An approach to computing electrostatic charges for molecules. *J. Comput. Chem.* **1984**, *5*, 129−145.
(33) Frisch, M. J.; Trucks, G. W.; Schlegel, H. B.; Scuseria, G. E.; Robb, M. A.; Cheeseman, J. R.; Zakrzewski, V. G.; Montgomery, J. A., Jr.; Stratmann, R. E.; Burant, J. C.; Dapprich, S.; Millam, J. M.; Daniels, A. D.; Kudin, K. N.; Strain, M. C.; Farkas, O.; Tomasi, J.; Barone, V.; Cossi, M.; Cammi, R.; Mennucci, B.; Pomelli, C.; Adamo, C.; Clifford, S.; Ochterski, J.; Petersson, G. A.; Ayala, P. Y.; Cui, Q.; Morokuma, K.; Malick, D. K.; Rabuck, A. D.; Raghavachari, K.; Foresman, J. B.; Cioslowski, J.; Ortiz, J. V.; Baboul, A. G.; Stefanov, B. B.; Liu, G.; Liashenko, A.; Piskorz, P.; Komaromi, I.; Gomperts, R.; Martin, R. L.; Fox, D. J.; Keith, T.; Al-Laham, M. A.; Peng, C. Y.; Nanayakkara, A.; Challacombe, M.; Gill, P. M. W.; Johnson, B.; Chen, W.; Wong, M. W.; Andres, J. L.; Gonzalez, C.; Head-Gordon, M.; Replogle, E. S.; Pople, J. A. *Gaussian 98*, Revision A.9; Gaussian, Inc.: Pittsburgh, PA, 1998.
(34) Bush, B. L.; Nachbar, R. B. Sample-distance partial least squares: PLS optimized for many variables, with application to CoMFA. *J. Comput.-Aided Mol. Des.* **1993**, *7*, 587−619.

(35) Widler, L.; Jaeggi, K. A.; Glatt, M.; Muller, K.; Bachmann, R.; Bisping, M.; Born, A. R.; Cortesi, R.; Guiglia, G.; Jeker, H.; Klein, R.; Ramseier, U.; Schmid, J.; Schreiber, G.; Seltenmeyer, Y.; Green, J. R. Highly potent geminal bisphosphonates. From pamidronate disodium (Aredia) to zoledronic acid (Zometa). *J. Med. Chem.* **2002**, *45*, 3721−3738.

(36) Soloducho, J.; Gancarz, R.; Wieczorek, P.; Korf, J.; Hafner, J.; Lejczak, B.; Kafarski, P. Method of obtaining novel derivatives of aminomethylene bisphosphonic acid. Polish Patent PL172268B, Aug 29, 1997.

(37) Martin, M. B.; Grimley, J. S.; Lewis, J. C.; Heath, H. T., III; Bailey, B. N.; Kendrick, H.; Yardley, V.; Caldera, A.; Lira, R.; Urbina, J. A.; Moreno, S. N.; Docampo, R.; Croft, S. L.; Oldfield, E. Bisphosphonates inhibit the growth of *Trypanosoma brucei*, *Trypanosoma cruzi*, *Leishmania donovani*, *Toxoplasma gondii*, and *Plasmodium falciparum*: a potential route to chemotherapy. *J. Med. Chem.* **2001**, *44*, 909−916.

(38) Ghosh, S.; Chan, J. M. W.; Lea, C. R.; Meints, G. A.; Lewis, J. C.; Tovian, Z. S.; Flessner, R. M.; Loftus, T. C.; Bruchhaus, I.; Kendrick, H.; Croft, S. L.; Kemp, R. G.; Kobayashi, S.; Nozaki, T.; Oldfield, E. Effects of bisphosphonates on the growth of *Entamoeba histolytica* and *Plasmodium* species *in vitro* and *in vivo*. *J. Med. Chem.*, in press.

(39) Takeuchi, M.; Sakamoto, S.; Kawamuki, K.; Kurihara, H.; Nakahara, H.; Isomura, Y. Studies on novel bone resorption inhibitors. II. Synthesis and pharmacological activities of fused aza-heteroaryl bisphosphonate derivatives. *Chem. Pharm. Bull.* **1998**, *46*, 1703−1709.

(40) Hutchinson, D. W.; Thornton, D. M. Michael addition reactions of ethenylidenebisphosphonates. *J. Organomet. Chem.* **1988**, *346*, 341−348.

(41) Mikhalin, N. V.; Alferev, I. S.; Kotlyarevskij, I. L.; Krasnukhina, A. V. Method of preparation of higher 1-hydroxyalkylidene-1,1-diphosphonic acids or their mixtures or salts. Russian Patent SU1719405, March 15, 1992.

(42) Benedict, J. J.; Perkins, C. M. Methods of treating diseases with certain geminal diphosphonates. United States Patent 4902679, Feb 20, 1990.

(43) Morita, C. T.; Verma, S.; Aparicio, P.; Martinez, C.; Spits, H.; Brenner, M. B. Functionally distinct subsets of human $\gamma\delta$ T cells. *Eur. J. Immunol.* **1991**, *21*, 2999−3007.

(44) *Prism*, version 3; Graphpad Software, 11452 El Camino Real, San Diego, CA 92130.

(45) Dunford, J. E.; Thompson, K.; Coxon, F. P.; Luckman, S. P.; Hahn, F. M.; Poulter, C. D.; Ebetino, F. H.; Rogers, M. J. Structure−activity relationships for inhibition of farnesyl diphosphate synthase *in vitro* and inhibition of bone resorption *in vivo* by nitrogen containing bisphosphonates. *J. Pharmacol. Exp. Ther.* **2001**, *296*, 235−242.

(46) Brown, R. J.; Van Beek, E.; Watts, D. J.; Löwik, C. W. G. M.; Papapoulos, S. E. Differential effects of aminosubstituted analogs of hydroxy bisphosphonates on the growth of *Dictyostelium discoideum*. *J. Bone Miner. Res.* **1998**, *13*, 253−258.

(47) *Viewer Lite*, version 5.0; Accelrys Inc., 9685 Scranton Rd., San Diego, CA 92121.

(48) Gossman, W.; Oldfield, E. Quantitative structure−activity relations for $\gamma\delta$ T cell activation by phosphoantigens. *J. Med. Chem.* **2002**, *45*, 4868−4874.

(49) Szabo, C. M.; Oldfield, E. An investigation of bisphosphonate inhibition of a vacuolar proton-pumping pyrophosphatase. *Biochem. Biophys. Res. Commun.* **2001**, *287*, 468−473.

JM0303709